A FIRST LOOK AT THE CLOUDSAT LIGHT PRECIPITATION DATASET

T. S. L'Ecuyer[1], S. D. Miller[2], C. Mitrescu[2], J. M. Haynes[1], C. Kummerow[1], and F. J. Turk[2]

[1]Colorado State University
Fort Collins, Colorado

[2]Naval Research Laboratory
Monterey, California

ABSTRACT

While significant progress has been made in satellite-based precipitation measurement, light liquid precipitation and falling snow are poorly sampled by current instruments but may represent a significant component of total precipitation particularly at latitudes poleward of 40 degrees. Since its launch in April, CloudSat's millimeter wavelength cloud radar has produced spectacular high resolution images of a wide range of precipitating clouds ranging from shallow, isolated convection to frontal systems and even deep convection clearly illustrating its capability to detect rainfall under most circumstances. Furthermore, a first look at light rainfall retrievals from data acquired during CloudSat's first few months of operation has yielded encouraging evidence of the potential utility of light precipitation products that will soon be in routine production within the Naval Research Laboratory's Near-Realtime Processing System (NRTPS). A cursory investigation of the statistical properties of rainfall systems at mid-high latitudes generated from these early CloudSat products will be presented with an eye toward subsequent analysis of the assumptions governing rainfall retrievals from the AMSR-E instrument aboard the Aqua satellite. While very preliminary in nature, the results demonstrate the unique opportunity CloudSat's observations provide for performing a global survey of light rainfall and snowfall, to quantify their contribution to the global water cycle, and to assess the performance of more traditional satellite-based rainfall retrieval techniques.

1. INTRODUCTION

Rainfall and snowfall provide dynamic reservoirs for liquid and ice in the atmospheric branch of the hydrologic cycle and represent by far the most dominant source of fresh water for agriculture and human consumption. In spite of recent advances in sensor technology such as the sensors aboard the Tropical Rainfall Measuring Mission (TRMM), there remain several key areas of space-based precipitation retrieval that are not well understood. PMW retrievals which are generally considered the most trustworthy source of global precipitation information, for example, rely heavily on the lower frequency channels (6-19 GHz, depending on the sensor) where the on-Earth resolutions are the coarsest (e.g. 40 km in the case of TRMM Microwave Imager, TMI). Furthermore, due to the fundamental path-integrated nature of a passive measurement, there is an uncertainty associated with the discrimination of precipitating and non-precipitating cloud. This leads to uncertainty in both the up-front screening of a rain/no-rain pixel(s) and the retrieved intensity. Over land, PMW retrievals are inhibited by the radiometrically warm surface emissivity, which varies widely both spatially and temporally, especially for light precipitation rates and snow-covered or cold surfaces, inhibiting the use of emission-based channels. Light rainfall also presents a problem to spaceborne precipitation radar technology. The lightest precipitation detectable by the TRMM PR, for example, is ~0.7 mm h^{-1} (more or less independent of surface

type), assuming a Z-R relationship appropriate to tropical precipitation and that the entire 4 km footprint of the PR is filled with rain (Iguchi et al., 2000).

Snowfall poses an even greater challenge to both spaceborne PMW sensors and radars producing only a scattering signal at the highest PMW frequencies while being all but invisible at the wavelength of the PR. Thus, while current rainfall sensors likely capture a majority of the moderate to heavy precipitation that dominates the Tropics, a significant fraction of lighter precipitation at higher latitudes may be missed. This point is illustrated in Fig. 1, which presents the fractions of zonally averaged precipitation accumulation that falls in the form of liquid precipitation lighter than 1 mm h^{-1} and snowfall derived from the Comprehensive Ocean-Atmosphere Data Set (COADS) ship-borne meteorological observations between 1958 and 1991. While this dataset is by no means intended to represent the true zonal distribution of these types of precipitation, it does suggest that a significant fraction of the precipitation that falls at latitudes poleward of 30^{o} and, in turn, a large fraction of the fresh water in these regions derives from forms of precipitation that are near or below the thresholds of detection of these instruments. Regrettably, for light precipitation over the global oceans there is scant and incomplete validation data from which to quantify how much of the rain distribution we are effectively capturing. This paper provides an overview of the anticipated role CloudSat (Stephens et al, 2002) observations may play in quantifying the global distribution of light rainfall, and snowfall and their variability on synoptic and seasonal timescales providing a unique opportunity to study their role in global climate change.

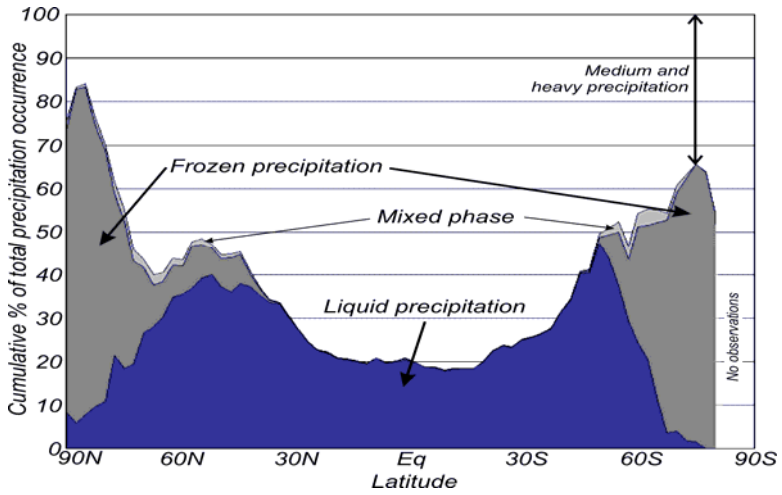

Figure 1: Frequency of occurrence of light rainfall (less than 1 mm h^{-1}) and snowfall from the COADS dataset (courtesy C. Kidd).

2. LIGHT PRECIPITATION FROM CLOUDSAT'S PERSPECTIVE

CloudSat and the Cloud-Aerosol Lidar and Infrared Pathfinder Satellite Observations (CALIPSO) satellites were successfully launched from Vandenberg Air Force Base in California on April 26, 2006. Shortly thereafter these satellites joined Aqua in a sun-synchronous orbit at an altitude of 705 km with an equatorial crossing time of 1:30 pm local time in the ascending mode of their orbits. From the moment it was activated on May 20, 2006, the 94 GHz CloudSat Cloud Profiling Radar (CPR) has provided an unprecedented view of the vertical structure of clouds around the

planet. From the very beginning, the CPR has also provided a unique perspective on light precipitation around the planet as evidenced by Figure 2 that depicts the first image acquired by CloudSat. The upper panel illustrates that the observations were acquired over the North Sea while the lower panel presents a 1300 km vertical cross section of observed radar reflectivity for this segment. The image clearly depicts a variety of high and low clouds along with a large (~200 km) precipitation feature that extends from the surface to about 10 km in height. While Figure 2 does not in any way present quantitative retrieval results, this first image acquired by the CPR provided strong motivation for developing the rainfall products for CloudSat that will be described in Sections 3 and 4. Other images like these (eg. Figure 5) provided evidence of CloudSat's sensitivity to frozen precipitation further motivating the development of the quantitative snowfall retrieval algorithm discussed in Section 5.

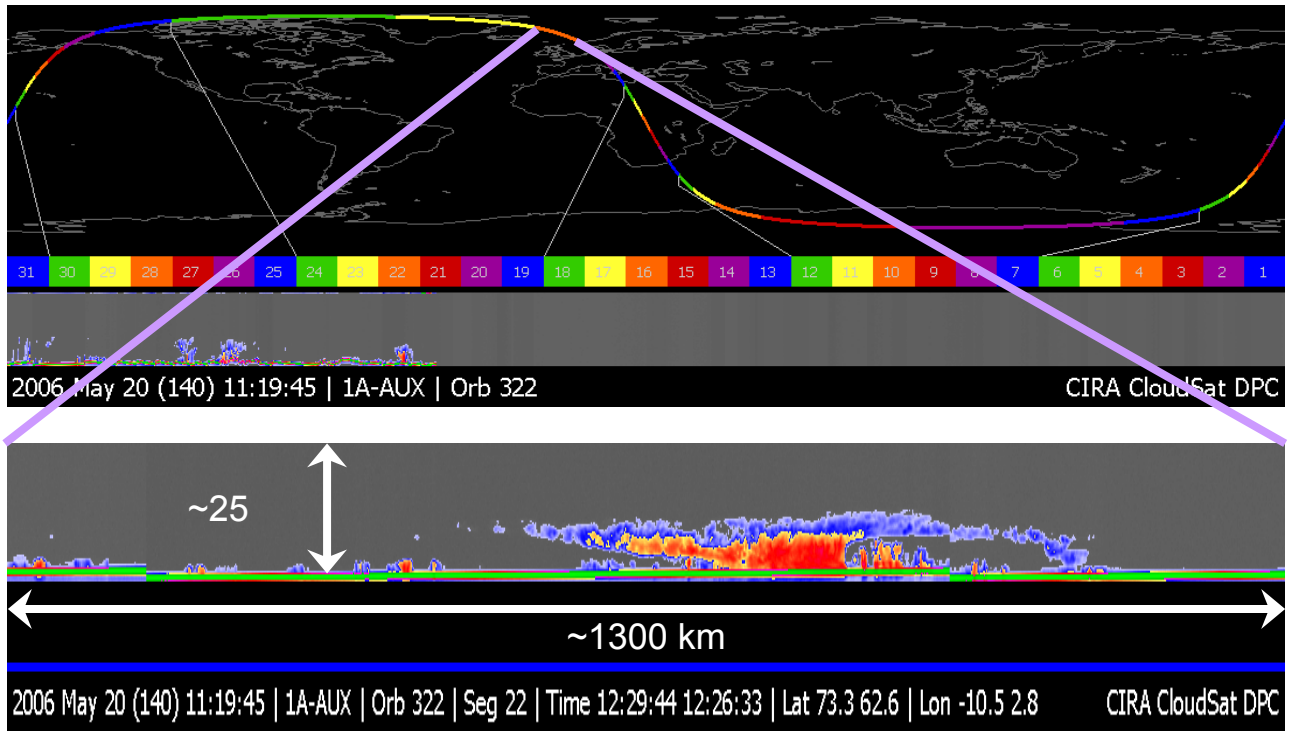

Figure 2: CloudSat's "first image" acquired May 20, 2006.

3. LIGHT RAINFALL RETRIEVALS

The suite of algorithms developed for CloudSat have been designed to both take advantage of complementary information from the other sensors on the A-Train, such as AMSR-E and MODIS radiance data from Aqua, and to provide rigorously-derived estimates of the uncertainties in each product. Following this mold, the CloudSat light rainfall algorithm has been formulated in the optimal estimation framework (Rodgers, 2000) that explicitly accounts for uncertainties in all sources of input data and propagates these uncertainties through the retrieval physics to supply corresponding estimates of the uncertainties in all retrieved products. In addition, the algorithm has been formulated with the capability of including a precipitation water path constraint from AMSR-E. Due to the strong attenuation of precipitation-sized hydrometeors at 94 GHz, the rainfall algorithm also requires an integral constraint in the form of the Path Integrated Attenuation (PIA) to unambiguously retrieve rainfall rate. Additional details of the algorithm can be found in L'Ecuyer

and Stephens (2002) or a corresponding paper from the previous IPWG precipitation workshop L'Ecuyer et al. (2004).

This algorithm has been implemented at the Naval Research Laboratory on its near real-time processing system (NRTPS). The NRTPS was established to handle multisensor (currently, 23 optical and microwave environmental satellite sensors from a constellation of 13-polar orbiting and 6-geostationary platforms) and model fusion (from the Navy global and mesoscale prediction systems) processing within a research and development framework. While NRL's commitment to operational transition of its research deliverables to a great extent necessitates such a system, its benefits extend beyond the facilitation of transition. During Operation Iraqi Freedom, NRL exploited the NRTPS in providing satellite meteorology support (e.g., dust, rainfall, fire, cloud properties, snow, and high resolution true color imagery) directly to DoD and Coalition assets within a timeframe useful for a wide variety of applications that included mission planning, ship navigation, and target/weaponry selection (Miller et al., 2005). Level-1B CPR data (calibrated cloud reflectivity) are ingested within an average of 6 hrs of being collected enabling the staging of these data upon the NRPTS with the full complement of contemporary satellite/model digital datasets. The retrieval is performed on all pixels determined to be cloudy by the CloudSat geometric profile product (GEOPROF) that is run as a preprocessing step. Ancillary data (e.g., global temperature/moisture profiles, surface winds, and surface temperatures) are supplied from the Navy Operational Global Atmospheric Prediction System (NOGAPS). These data are used to compute the component of attenuation due to atmospheric gaseous absorption as well as to define the surface wind speed needed to estimate the expected clear-sky surface return required to estimate PIA.

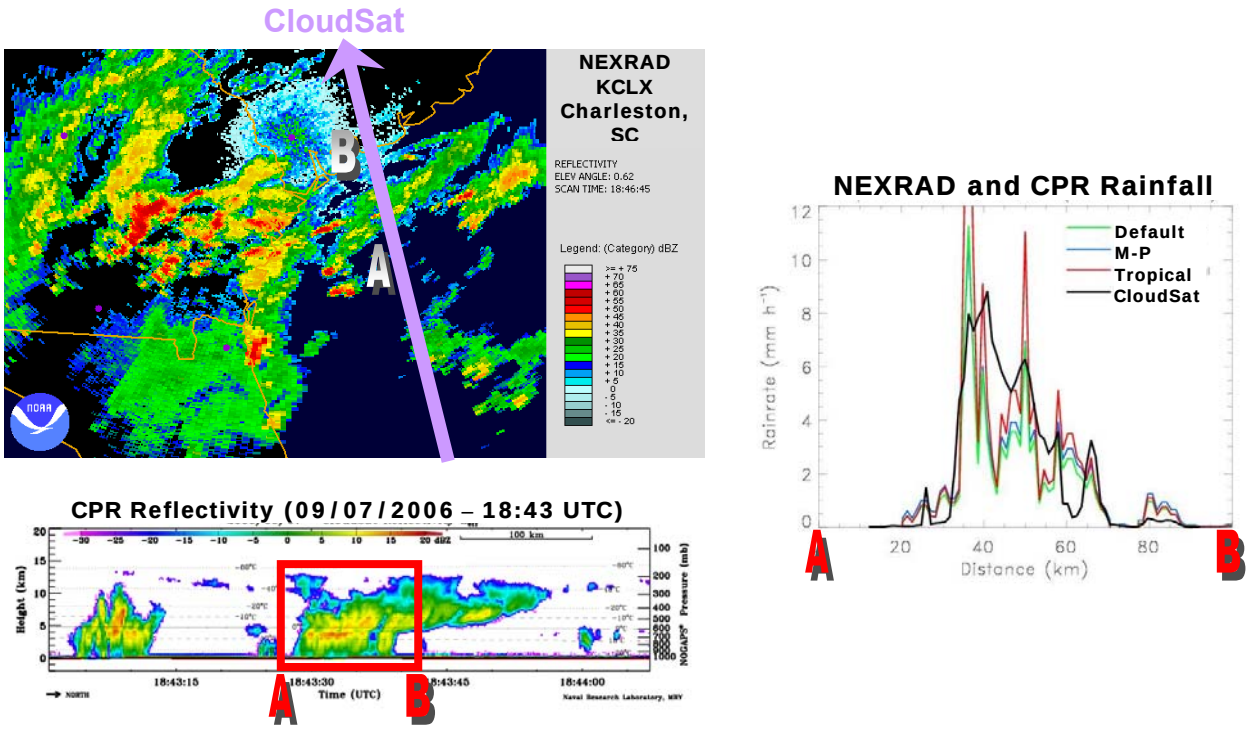

Figure 3: Early rainfall retrieval from CloudSat. The upper left hand panel shows the lowest scan of the Charleston NEXRAD radar (KCLX) with the CloudSat ground track superimposed. The lower left hand panel shows corresponding reflectivities observed by the CPR. The panel on the right shows retrieved rainfall from CloudSat (black curve) along with three different rainfall estimates from the NEXRAD radar derived using three distinct Z-R relationships.

An example of a rainfall retrieval from a precipitation system off the coast of South Carolina is shown in Figure 3. The scene consists of several rain bands with embedded convective cores between 10 and 15 km deep two of which were intersected by CloudSat. The CloudSat reflectivity cross-section indicates a smaller developing convective cell on the left followed by a larger area of more mature precipitation characterized by thick cirrus cloud overlying a persistent area of moderate rainfall with a well-defined melting level at ~4.5 km. Reflectivities exceeding 10 dBZ throughout most of the scene indicate the presence of large precipitating liquid and ice particles and the decrease in reflectivity in the rainfall between the melting level and the surface is indicative of their strong attenuation at 94 GHz. Retrieved surface rainfall rate for the indicated region is presented on the right and compared with similar estimates from the NEXRAD data themselves. Retrieved rainrates range from less than 1 to above 10 mm h^{-1} across the scene and those from CloudSat (black curve) generally agree with those from the ground radar to within the uncertainty expected from using three different standard NEXRAD Z-R relations that may be appropriate for this region (colored curves). Subtle differences in the precise location and magnitude of intensity peaks may also be a result of imperfect time/space matching of the two datasets as well as differences in the sample volumes of the two instruments. While this in no way guarantees that the CloudSat rainfall estimates are quantitatively accurate, it provides a reassuring sanity check that the results are in line with those obtained by more traditional precipitation sensors and further motivates the generation of a standard CloudSat light rainfall product. This example also serves to illustrate the fact that despite the strong attenuation at 94 GHz, CPR observations may be capable of retrieving rainfall out to higher intensities than previously thought. Here the CloudSat algorithm is capable of capturing rainfall rates exceeding 10 mm h^{-1} with no sign of degradation due to the corresponding attenuation provided it is modeled correctly.

4. COMPARISON WITH AMSR-E

It has already been noted above that the nature of the PMW rainfall signature poses a challenge at in light precipitation due to the difficulty associated with discriminating cloud from rain. This is particularly true when the freezing level is low and the vertical extent of the liquid water is shallow. The low horizontal resolution of PMW sensors also lead to uncertainty in rainfall estimates in scenes with significantly variable precipitation. By virtue of its 240m vertical and 1.4 km horizontal resolution, the CPR offers an opportunity to examine rainfall systems at a much higher resolution than afforded by PMW sensors. In addition, it's strong sensitivity to particle size, particularly in very light precipitation, makes CloudSat an ideal sensor for accurately determining precipitation occurrence. On the other hand, this high sensitivity to drop size can lead to large uncertainties in rainfall intensity. It is, therefore, of great interest to exploit the coincident observations of CloudSat and the AMSR-E instrument aboard Aqua in an effort to better understand the magnitudes of the dominant sources of uncertainty suffered by each.

Preliminary comparisons of rainrate histograms from carefully matched CPR and AMSR-E observations are presented in Figure 4 for a 16 day period in August, 2006. Two regions are highlighted consisting of the zonal belt between 10ºN and 10ºS and another from 40ºS and 60ºS to contrast tropical precipitation with that found at higher latitudes in winter. While very preliminary in nature and covering only a very short duration, even these initial rainfall PDFs illustrate the challenges faced by PMW sensors at higher latitudes. The sensors agree reasonably well in the tropics with AMSR-E retrieving slightly more light rainfall and CloudSat retrieving a number of heavier events consistent with the higher spatial resolution of the latter. Between 40ºS and 60ºS, however, where the freezing level is typically between 1 and 2 km at this time of year, the AMSR-E identifies significantly fewer rainfall events than CloudSat, presumably due to the LWP threshold

used for rain/no-rain discrimination. While no rigorous conclusions should be drawn from these early results, they do point to a potentially valuable contribution that CloudSat observations may make in assessing the rainfall discrimination capabilities of PMW sensors.

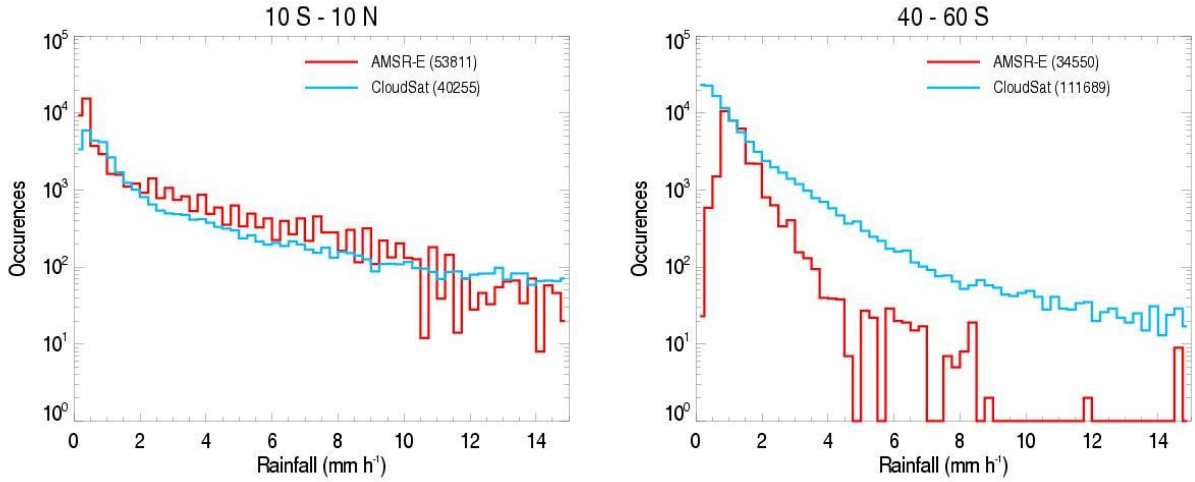

Figure 4: Preliminary comparison of rainfall statistics from CloudSat (red) and the AMSR-E instrument aboard Aqua (red). Statistics in two 20º zonal belts are shown: one centered on the equator (left) and the other from 40-60ºS.

5. FROZEN PRECIPITATION

Snowfall is common during the winter months at the mid and high latitudes and represents a significant fraction of the fresh water used for consumption and agriculture in these regions measuring snowfall from current satellite-based precipitation sensors has been difficult due to challenges associated with distinguishing falling snow from that on the surface. CloudSat reflectivities will provide a means for detecting this snowfall and may allow quantitative retrievals of falling snow particularly when combined with the high frequency (89 GHz) channel of AMSR-E. This possibility is also being explored using the optimal estimation approach described above. In this case, the CPR reflectivity measurements are used to retrieve the width parameter and number concentration of an exponential distribution of spherical snow particles.

This algorithm has been applied to a snowfall scene acquired by CloudSat on August 29, 2006 off the coast of Antarctica shown in Figure 5. The scene consists of a widespread area of variable snowfall approximate 400 km long just off the coast of Antarctica (note the coast can just been seen on the far right hand side of the bottom of the lower panel of Figure 5 depicted in brown). Reflectivities range from 0-10 dBZ and the cloud layer ranges in thickness from 2-5 km with evidence of some relatively heavy snow bands embedded in the system. Corresponding profiles of retrieved width parameter, Λ, and column-mean number density, N_0, for the exponential particle size distribution, $N(D) = N_0 e^{-\Lambda D}$, are presented in Figure 6 along with an associated snowfall rate derived by assuming an appropriate fall velocity-particle size relationship. The largest particles are concentrated in the regions of strongest reflectivity as expected and these regions give rise to the largest snowfall rates as indicated in the bottom panel. Unfortunately due to the remote nature of this region, no information exists for validation purposes. Evaluation of the performance of this algorithm, therefore, remains a topic for future study and a field experiment is planned in southern

Ontario, Canada between October 2006 and March 2007 that will specifically address this issue. The need for validation and further refinements notwithstanding, these results once again serve to illustrate the potential for using CloudSat measurements to detect snowfall and possibly even infer its intensity on the global scale.

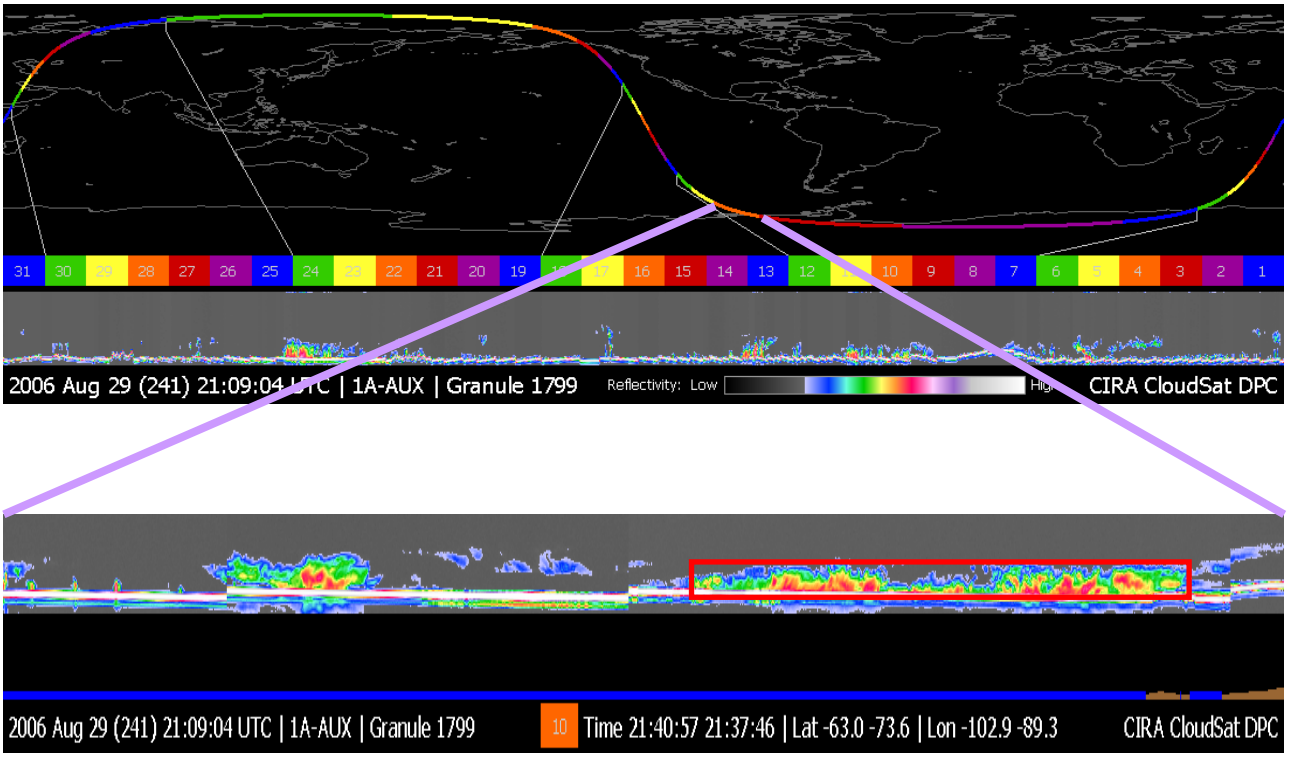

Figure 5: A snowfall scene observed by CloudSat off the coast of Antarctica.

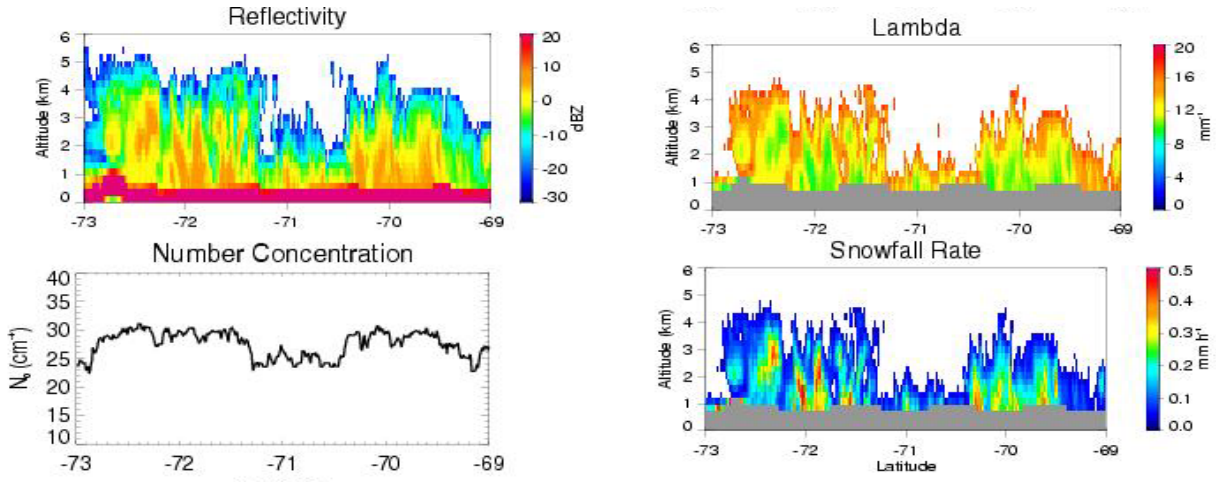

Figure 6: Preliminary snowfall retrieval from CloudSat. Reflectivities from the scene depicted in Figure 5 have been reproduced in the upper left panel. The remaining panels show retrieved number concentration, width parameter, Λ, and implied snowfall rate, respectively.

6. DISCUSSION

Early results from the application of two new precipitation algorithms to data acquired during CloudSat's first few months of operation confirm its potential for quantifying the role played by light rainfall and snow in the global water cycle. It is important to emphasize that neither of these algorithms has undergone any formal validation but it is encouraging that the results are reasonable given the regions examined and time of year. With the growing amount of field data being acquired in support of CloudSat's validation program, extensive evaluation of both the rainfall and snowfall estimates and their uncertainty estimates are planned for the near future. It is anticipated that these products will continue to be refined and improved in the coming year and will ultimately form the basis of enhanced science products for the CloudSat mission that will be made available to the science community through the CloudSat Data Processing Center (http://www.cloudsat.cira.colostate.edu/dpcstatusTrack.php) in late 2007 or early 2008.

The over-arching goal of the A-Train constellation is to provide a synergistic view of the primary components of the global hydrologic cycle and energy budget including water vapor, clouds, rainfall, aerosols, and the distribution of various chemical species in the atmosphere as well as longwave and shortwave radiative fluxes at the top of the atmosphere. In this broader context, CloudSat's rainfall products open up a number of avenues for further research related to the combination of information from complementary sensors in the constellation. While CloudSat's primary role in the A-Train will continue to be as a source of information concerning the vertical distribution of liquid and ice water content, the ability of the CPR to simultaneously detect liquid clouds, ice clouds, light liquid rainfall, and snowfall will offer insight into processes of fundamental importance to understanding the role of clouds and light precipitation in the large-scale environment. Of particular interest from a climate perspective are the mechanisms for rainfall formation, the processes by which aerosols modify clouds and precipitation, and the resulting implications for the global energy and water cycle. The products introduced here in combination with those from other A-Train sensors, therefore, have the potential to both improve our ability to predict the weather and advance our understanding of several key climatic processes.

6. REFERENCES

L'Ecuyer, T. S. and G. L. Stephens, 2002: An estimation-based precipitation retrieval algorithm for attenuating radars, *J. Appl. Meteor.* **41**, 272-285.

L'Ecuyer, T. S., 2004: Experimental light rainfall and snowfall products for CloudSat, *2nd International Precipitation Working Group Workshop on Precipitation Measurements*, Monterey, CA, 298-305.

Miller, S. D. and co-authors 2006: MODIS provides a satellite focus on Operation Iraqi Freedom, *Int. J. Rem. Sens.*, in press.

Rodgers, C. D., 2000: Inverse methods for atmospheric sounding. Theory and practice., World Scientific, Singapore, 2000.

Stephens, G. L. and co-authors, 2002: The CloudSat mission and the A-Train: A new dimension of space-based observations of clouds and precipitation, *Bull. Amer. Meteor. Soc.* **83**, 1771-1790.